Journal of Computational Mathematics
Vol.xx, No.x, 2025, 1–20.
http://www.global-sci.org/jcm
doi:10.4208/jcm.2412-m2024-0126

A POSTERIORI ERROR ESTIMATES OF THE WEAK GALERKIN FINITE ELEMENT METHOD FOR POISSON-NERNST-PLANCK EQUATIONS*

Wanwan Zhu
School of Mathematics and Statistics, Guangdong University of Technology, Guangzhou 510520, China;
School of Mathematical Sciences, Beijing Normal University, Laboratory of Mathematics and Complex Systems, Ministry of Education, Beijing 100875, China
Email: zhuww@gdut.edu.cn
Guanghua Ji[1)]
School of Mathematical Sciences, Beijing Normal University, Laboratory of Mathematics and Complex Systems, Ministry of Education, Beijing 100875 China
Email: ghji@bnu.edu.cn

Abstract

In this paper, we present a posteriori error estimates of the weak Galerkin finite element method for the steady-state Poisson-Nernst-Planck equations. The a posteriori error estimators for the electrostatic potential and ion concentrations are constructed. The reliability and efficiency of the estimators are verified by the upper and lower bounds of the energy norm of the error. The a posteriori error estimators are applied to the adaptive weak Galerkin algorithm for triangle, quadrilateral and polygonal meshes with hanging nodes. Finally, numerical results demonstrate the effectiveness of the adaptive algorithm guided by our constructed estimators.

Mathematics subject classification: 65N15, 65N30.
Key words: A posteriori error estimate, Weak Galerkin finite element method, Poisson-Nernst-Planck equations, Adaptive weak Galerkin algorithm, Polygonal meshes.

1. Introduction

The Poisson-Nernst-Planck (PNP) equations, which describe the diffusion process of ions under the action of an electric field, are well-known ion transport models and play a crucial role in the study of many physical and biological phenomena. Since the PNP equations were proposed, their mathematical analysis and numerical approximation have attracted extensive attention. The existence of solutions to the PNP equations has been presented in [21, 24]. Due to the nonlinear coupling of PNP equations, it is challenging to compute their analytical solutions mathematically. Therefore, numerical methods are usually used to find approximate solutions [13, 17, 39]. PNP equations in some practical problems, such as ion channels [6, 31], have singularity due to many charges on the membrane interface, and the accuracy of their approximate solutions largely depends on the quality of the mesh. If the discrete mesh is not good, numerical methods such as the finite element method cannot effectively solve the PNP

* Received June 27, 2024 / Revised version received November 16, 2024 / Accepted December 2, 2024 / Published online January 6, 2025 /
1) Corresponding author

equations. In this case, the adaptive algorithm driven by an a posteriori error estimator is a good choice to improve the efficiency of mesh generation.

The a posteriori error estimator is the basis of the adaptive algorithm. As a computable quantity, the a posteriori error estimator can guide adaptive mesh refinement so that the adaptive algorithm can obtain more accurate numerical solutions with fewer mesh degrees of freedom. At present, there are some works on solving PNP equations by adaptive algorithms. In [32, 37], the adaptive algorithm is applied to solve the actual ion channel problem described by the PNP equations. However, in the adaptive algorithm, only the a posteriori error estimator of the Poisson equation in PNP equations is used to guide the adaptive mesh refinement, and the influence of the NP equation is not considered. The gradient recovery-type a posteriori error for a class of steady-state PNP equations is derived in [29], and its error estimator is proven to be efficient and reliable. Then, by using a local averaging operator which is an extension of the gradient recovery operator, the locally averaged a posteriori error estimate for the nonlinear PNP problem is derived in [40]. In [16], a spatial adaptive finite element method considering geometrical singularities and boundary layer effects is proposed for the steady-state PNP equations. In [46], the residual-type a posteriori error estimate for time-dependent PNP equations is studied, the error estimators are established and the computable upper and lower bounds of the error estimators are derived. These works utilizing adaptive algorithms to solve PNP equations are suitable for regular triangular or tetrahedral meshes only. To eliminate the hanging nodes created in adaptive mesh refinement, the traditional finite element method needs to refine additional elements, resulting in higher shape regularity conditions [33], which cannot be directly applied to polygonal meshes. With the improvement of computing power and numerical calculation levels, PNP equations have been applied to simulate large-scale systems, such as actual biology and physics [3, 38], in recent years, but the cost of computing on traditional structured meshes is relatively expensive. Adaptive computation on polygonal meshes allows the existence of hanging points, and no postprocessing is needed to refine the meshes. If the mesh in the adaptive algorithm has great flexibility, the mesh refinement strategy can be implemented more effectively. Hence, the convenient use of more general polygonal meshes in complex simulations has become an attractive feature.

Here, we design a posteriori error estimators of the weak Galerkin finite element method for steady-state PNP equations. The weak Galerkin finite element method (WGFEM) is a new numerical method developed in recent years to solve various partial differential equations. It was first proposed by Mu, Wang and Ye [27, 34, 35] for solving second-order elliptic problems. The WGFEM can be seen as an extension of the standard finite element method, and its finite element discrete scheme can be derived directly from the weak form of the corresponding PDE. The scheme for WGFEM is constructed by using fully discontinuous finite element functions. Therefore, compared with other finite element methods, it has the advantages of flexible approximation functions, a simple and stable numerical scheme, and can deal with unstructured meshes [20, 26]. The WGFEM has developed rapidly since it was proposed and has been applied to solve many problems [5, 8, 22, 30, 36, 41, 42]. Based on the WG-mixed finite element method (MFEM), a linearized locally conservative scheme for time-dependent PNP equations is established in [14], and the prior error estimates of semidiscrete and fully discrete WG-MFEM schemes are given. There are also some works about a posteriori error estimators for the WGFEM [4, 43–45]. However, the adaptive computations of these works are carried out on regular triangular mesh or tetrahedral mesh. Recently, there have been some research works devoted to the a posteriori error analysis of WGFEM on general polygonal or polyhedral meshes [1, 2, 19, 23, 25], but these works are all about linear problems, and as far as we know, there is no literature on the a posteriori error analysis of WGFEM for nonlinear problems.

In this paper, a posteriori error estimators of WGFEM are established for a class of steady-state PNP equations. Compared with the proposed works on a posteriori error estimation of PNP equations, the estimators have several characteristics:

1) Our error estimators are simple. Except for data oscillation and high-order quantities, they contain a parameterless stabilizer only. In our a posteriori error estimators, there are no common terms in the previous works on a posteriori error estimation, such as area residuals and flux jump.

2) Due to the simple composition of the a posteriori error estimators, we can directly obtain their lower bound estimation in theoretical analysis.

3) In adaptive computation, the main part of the a posteriori error estimators, namely, the stabilizers, have already been calculated when using WGFEM to solve the PNP equations. Therefore, when calculating a posteriori error estimators, the stabilizer can be used directly without additional cost.

4) The adaptive algorithm can be calculated on unstructured meshes such as arbitrary polygon/polyhedron meshes, mixed meshes and meshes with hanging points, so the adaptive mesh refinement does not need postprocessing. We construct a posteriori error estimators for the electrostatic potential and ion concentrations, respectively, and we give their upper and lower bounds analysis to prove the reliability and efficiency of the error estimators. Several adaptive computations on different polygonal meshes are presented to verify the theoretical analysis.

The outline of the paper is organized as follows. In Section 2, we introduce the definition of WG finite element space and develop the WG discrete scheme of the steady-state PNP equations. The a posteriori error estimators for the unknown solutions of electrostatic potential ϕ and ion concentrations p^i are constructed in Section 3 by using the WGFEM, and their reliability and efficiency are derived in the energy norm. In Section 4, we report the results of numerical tests on several different adaptive meshes to validate our theoretical results.

2. The Weak Galerkin Finite Element Method

2.1. Model problem

We consider a class of steady-state PNP equations with Dirichlet boundary conditions as follows:

$$-\nabla\cdot\nabla\phi=\sum_{i=1}^{2}q^ip^i+f_3 \qquad \text{in } \Omega, \tag{2.1}$$

$$-\nabla\cdot(\nabla p^i+q^ip^i\nabla\phi)=f_i, \quad i=1,2 \qquad \text{in } \Omega, \tag{2.2}$$

$$\phi=0, \quad p^i=0 \qquad \text{on } \partial\Omega, \tag{2.3}$$

where Ω is a polygonal or a polyhedral domain in $\mathbb{R}^d$ $(d=2,3)$ with boundary $\partial\Omega$. The index i represents different ionic species, p^i is the concentration of the i-th ionic species with charge q^i, ϕ is the electrostatic potential and $f_i, i=1,2,3$ are the reaction source terms. For simplicity of notation, in the following, we shall assume $d=2$. The results can be extended to three-dimensional space.

Let D be any open region with boundary ∂D. We adopt the standard notation $W^{s,r}(D)$ ($s \geq 0$) to denote the Sobolev space on D. When $r=2, W^{s,r}(D)=H^s(D)$ denotes a Hilbert space with the inner product $(\cdot,\cdot)_{s,D}$, norms $\|\cdot\|_{s,D}$ and seminorms $|\cdot|_{s,D}$. When $s=0, H^0(D)$ coincides with $L^2(D)$ equipped with the L^2-norm $\|\cdot\|_D$ and the inner product $(\cdot,\cdot)_D$. Furthermore, if $D=\Omega$, the subscript D is omitted. Let us define

$$(u,v)_\Omega = \int_\Omega uv\,dx, \quad \langle u,v\rangle_{\partial\Omega} = \int_{\partial\Omega} uv\,ds.$$

2.2. The weak Galerkin finite element space

Let $\mathcal{T}_h$ be a partition of the domain Ω consisting of elements that are closed and simply connected polygons in two dimensions or polyhedra in three dimensions satisfying a set of conditions specified in [28, 35]. We denote by $\mathcal{E}_h$ the set of all edges or flat faces in $\mathcal{T}_h$, and we let $\mathcal{E}_h^0 = \mathcal{E}_h \backslash \partial\Omega$ be the set of all interior edges or flat faces. For any element $K \in \mathcal{T}_h$ with interior K^0 and boundary ∂K, we denote by h_K the diameter for K and mesh size $h = \max_{K\in\mathcal{T}_h} h_K$. A weak function $v=\{v_0, v_b\}$ on K has two pieces, $v_0 \in L^2(K)$ and $v_b \in H^{1/2}(\partial K)$. The first piece represents the values of v in the interior K^0, and the second piece represents the values on the element boundary ∂K. The space of weak functions defined on K is given by

$$W(K) = \big\{v=\{v_0,v_b\} : v_0 \in L^2(K), v_b \in H^{\frac{1}{2}}(\partial K)\big\}.$$

The weak gradient defined in [34] is introduced as follows.

Definition 2.1. *The weak gradient $\nabla_w v$ of a weak function $v \in W(K)$ is defined as a linear functional in the dual space of $[H^1(K)]^2$ satisfying*

$$(\nabla_w v, \boldsymbol{q})_K = -(v_0, \nabla\cdot\boldsymbol{q})_K + \langle v_b, \boldsymbol{q}\cdot\mathbf{n}\rangle_{\partial K}, \quad \forall\, \boldsymbol{q} \in [H^1(K)]^2, \tag{2.4}$$

where $\mathbf{n}$ is the outward unit normal vector of K.

If the components of $v=\{v_0,v_b\}$ are restrictions of a function $u \in H^1(K)$ on K^0 and ∂K, respectively, then for $\mathbf{q} \in [H^1(K)]^2$, we have

$$\begin{aligned}(\nabla_w v, \mathbf{q})_K &= -(v_0, \nabla\cdot\mathbf{q})_K + \langle v_b, \mathbf{q}\cdot\mathbf{n}\rangle_{\partial K}\\ &= -(u, \nabla\cdot\mathbf{q})_K + \langle u, \mathbf{q}\cdot\mathbf{n}\rangle_{\partial K} = (\nabla u, \mathbf{q})_K.\end{aligned}$$

It follows that $\nabla_w v = \nabla u$ is the classical gradient of u, if $u \in H^1(K)$.

For a given integer $k \geq 1$, let V_h be the WG finite element space associated with $\mathcal{T}_h$ defined as follows:

$$\begin{aligned}&V_h = \{v=\{v_0,v_b\} \,:\, v_0|_K \in P_k(K),\, v_b|_{\partial K} \in P_k(\partial K),\, K \in \mathcal{T}_h\},\\ &V_h^0 = \{v=\{v_0,v_b\} \in V_h, v_b|_{\partial K \bigcap \partial\Omega} = 0,\, \forall\, K \in \mathcal{T}_h\},\end{aligned}$$

where $P_k(K)$ is the set of polynomials with a degree no more than k on K. We want to emphasize that any function $v \in V_h$ has a single value v_b on each edge $\partial K \in \mathcal{E}_h$. We remark that the first component of v, namely, v_0, is the value of v in the interior of K^0, and the second component v_b is the single value on the edges of the boundary of K, which is not necessarily the trace of v_0 on the boundary. We adopt $[P_{k-1}(K)]^2$ as the discrete weak gradient space. Specifically, the definition of the discrete weak gradient in [34] can be described as follows.

Definition 2.2. *For a weak function $v = \{v_0, v_b\} \in V_h$, its discrete weak gradient $\nabla_{w,k-1}v \in [P_{k-1}(K)]^2$ satisfies*

$$(\nabla_{w,k-1}v, \boldsymbol{q})_K = -(v_0, \nabla \cdot \boldsymbol{q})_K + \langle v_b, \boldsymbol{q} \cdot \mathbf{n}\rangle_{\partial K}, \quad \forall\, \boldsymbol{q} \in [P_{k-1}(K)]^2. \tag{2.5}$$

For simplicity, we use ∇_w as the discrete weak gradient operator in the following analysis.

2.3. The discrete weak Galerkin scheme

The weak formulation of the system (2.1)-(2.3) is given as follows: Find $\phi \in H_0^1(\Omega)$ and $p^i \in H_0^1(\Omega), i = 1, 2$, such that

$$(\nabla\phi, \nabla w) - \sum_{i=1}^{2} q^i(p^i, w) = (f_3, w), \quad \forall\, w \in H_0^1(\Omega), \tag{2.6}$$

$$(\nabla p^i, \nabla v) + q^i(p^i \nabla\phi, \nabla v) = (f_i, v), \quad \forall\, v \in H_0^1(\Omega), \quad i = 1, 2. \tag{2.7}$$

To establish the WG discrete scheme, we define the following inner products:

$$\begin{aligned}
a_h(u, v) &= \sum_{K\in\mathcal{T}_h} (\nabla_w u, \nabla_w v),\\
b_h(u, v) &= \sum_{K\in\mathcal{T}_h} \sum_{i=1}^{2} q^i(u_0, v_0),\\
c_h(u, v, w) &= \sum_{K\in\mathcal{T}_h} q^i(u_0 \nabla_w v, \nabla_w w),\\
s_c(u, v) &= \sum_{K\in\mathcal{T}_h} h_K^{-1}\langle u_0 - u_b, v_0 - v_b\rangle_{\partial K},\\
s_d(u, v, w) &= \sum_{K\in\mathcal{T}_h} h_K^{-1} q^i \langle u_0(v_0 - v_b), w_0 - w_b\rangle_{\partial K}.
\end{aligned}$$

The WG discrete scheme for (2.6)-(2.7) is to find

$$\phi_h = \{\phi_{h,0}, \phi_{h,b}\} \in V_h^0, \quad p_h^i = \{p_{h,0}^i, p_{h,b}^i\} \in V_h^0, \quad i = 1, 2$$

such that

$$a_h(\phi_h, w_h) - b_h\big(p_h^i, w_h\big) + s_c(\phi_h, w_h) = (f_3, w_{h,0}), \qquad \forall\, w_h \in V_h^0, \tag{2.8}$$

$$a_h\big(p_h^i, v_h\big) + c_h\big(p_h^i, \phi_h, v_h\big) + s_c\big(p_h^i, v_h\big) + s_d\big(p_h^i, \phi_h, v_h\big) = (f_i, v_{h,0}), \quad \forall\, v_h \in V_h^0. \tag{2.9}$$

For the error functions $v_h \in V_h$, we introduce the following energy norm of WG finite element space:

$$|||v_h||| := \sqrt{a_h(v_h, v_h) + s_c(v_h, v_h)}. \tag{2.10}$$

It is not hard to see that $|||\cdot|||$ defines a seminorm in the finite element space V_h. We claim that this seminorm becomes a full norm in the finite element space V_h^0. Moreover, the following Poincaré-type inequality holds for functions in V_h^0.

Lemma 2.1 ([28]). *Let $\mathcal{T}_h$ be the finite element partition of Ω satisfying the shape regularity assumption. Then, for any $v_h \in V_h^0$, there exists a constant C independent of the mesh size h such that*

$$\|v_{h,0}\| \leq C|\!|\!|v_h|\!|\!|, \quad \forall\, v_h = \{v_{h,0}, v_{h,b}\} \in V_h^0. \tag{2.11}$$

In the finite element space V_h, we introduce a discrete H^1 seminorm as follows:

$$\|v_h\|_{1,h} = \left(\sum_{K\in\mathcal{T}_h} \left(\|\nabla v_{h,0}\|_K^2 + h_K^{-1}\|v_{h,0} - v_{h,b}\|_{\partial K}^2\right) \right)^{\frac{1}{2}}. \tag{2.12}$$

The following lemma indicates that $\|v_h\|_{1,h}$ is equivalent to the energy norm (2.10).

Lemma 2.2 ([27]). *There exist two positive constants C_1 and C_2 such that for any $v_h = \{v_{h,0}, v_{h,b}\} \in V_h$, we have*

$$C_1\|v_h\|_{1,h} \leq |\!|\!|v_h|\!|\!| \leq C_2\|v_h\|_{1,h}. \tag{2.13}$$

For each element $K \in \mathcal{T}_h$, we first define $Q_h v = \{Q_0 v, Q_b v\} \in V_h$ with Q_0 and Q_b be the L^2 projections from $L^2(K)$ to $P_k(K)$ and from $L^2(e)$ to $P_k(e)$, $e \subset \partial K$, respectively. Then, we denote by R_h the L^2 projection from $[L^2(K)]^2$ to a local weak gradient space $[P_{k-1}(K)]^2$.

Lemma 2.3 ([19]). *On each element $K \in \mathcal{T}_h$, we have the following commutative property for $v \in H^1(K)$:*

$$\nabla_w(Q_h v) = R_h(\nabla v), \tag{2.14}$$
$$\nabla_w v = R_h(\nabla v). \tag{2.15}$$

Lemma 2.4 ([28]). *Let $\mathcal{T}_h$ be a finite element partition of Ω that is shape regular. Then, for any $v \in H^{k+1}(\Omega)$, we have*

$$\sum_{K\in\mathcal{T}_h} \|v - Q_0 v\|_K^2 + \sum_{K\in\mathcal{T}_h} h_K^2\|\nabla(v - Q_0 v)\|_K^2 \leq Ch^{2(k+1)}\|v\|_{k+1}^2, \tag{2.16}$$
$$\sum_{K\in\mathcal{T}_h} \|\nabla v - R_h(\nabla v)\|_K^2 \leq Ch^{2k}\|v\|_{k+1}^2. \tag{2.17}$$

Let ϕ, p^i and $\phi_h = \{\phi_{h,0}, \phi_{h,b}\}$, $p_h^i = \{p_{h,0}^i, p_{h,b}^i\}$ be the solutions of (2.6)-(2.7) and (2.8)-(2.9), respectively. The L^2 projections of the solutions ϕ and p^i are given by

$$Q_h\phi = \{Q_0\phi, Q_b\phi\} \in V_h, \quad Q_h p^i = \left\{Q_0 p^i, Q_b p^i\right\} \in V_h.$$

Then, the errors between the L^2 projections of solutions ϕ, p^i and the WG approximation solutions ϕ_h, p_h^i are defined as

$$e_\phi = \{e_{\phi,0}, e_{\phi,b}\} = \{Q_0\phi - \phi_{h,0}, Q_b\phi - \phi_{h,b}\},$$
$$e_{p^i} = \{e_{p^i,0}, e_{p^i,b}\} = \left\{Q_0 p^i - p_{h,0}^i, Q_b p^i - p_{h,b}^i\right\}.$$

3. A Posteriori Error Analysis

In this section, the a posteriori error estimators are described and analyzed for the WG finite element scheme (2.8) and (2.9). For a scalar-valued function v, we define the curl operator by

$$\nabla \times v = \left(-\frac{\partial v}{\partial x_2}, \frac{\partial v}{\partial x_1}\right).$$

Let K be an element with e as an edge. The trace inequality is also used in the following estimation. It is well known that there exists a constant C such that, for any function $g \in H^1(K)$,

$$\|g\|_e^2 \le C\big(h_K^{-1}\|g\|_K^2 + h_K\|\nabla g\|_K^2\big). \tag{3.1}$$

The positive constant C is independent of mesh size h and can represent different values at different positions in this paper.

The following Helmholtz decomposition of an L^2 function is well known (cf. [9, p. 31], or [4]). Hence, we can easily obtain the following Helmholtz type decomposition of the function $\nabla u - \nabla_w u_h \in L^2(\Omega)$.

Lemma 3.1. *For $\nabla u - \nabla_w u_h \in L^2(\Omega)$, there exist $\psi \in H_0^1(\Omega)$ and $\Phi \in H^1(\Omega)$ such that*

$$\nabla u - \nabla_w u_h = \nabla\psi + \nabla \times \Phi, \tag{3.2}$$

$$\|\nabla u - \nabla_w u_h\|^2 = \|\nabla\psi\|^2 + \|\nabla \times \Phi\|^2. \tag{3.3}$$

Remark 3.1. In three dimensions, the vector potential $\psi \in H^1(\Omega)$ satisfying $\nabla u - \nabla_w u_h = \nabla\psi + \nabla \times \psi$ (cf. [15, p. 45]).

Let us define the following two local stabilizers on the edges of element K to simplify future proofs:

$$s_{c,K}(u,v) = h_K^{-1}\langle u_0 - u_b, v_0 - v_b\rangle_{\partial K}, \tag{3.4}$$

$$s_{d,K}(u,v,w) = h_K^{-1}q^i\langle u_0(v_0 - v_b), w_0 - w_b\rangle_{\partial K}. \tag{3.5}$$

3.1. Upper bound

In this subsection, we prove the reliability of the a posteriori error estimators for the electrostatic potential ϕ and the ion concentrations $p^i, i = 1, 2$; that is, the estimators provide the upper bounds on the true errors. Before proving the reliability of the a posteriori error estimators, we introduce the lemma developed in [19] to help with the analysis.

Lemma 3.2 ([19]). *For $u_h \in V_h^0$ and $\Phi \in H^1(\Omega)$, we have*

$$(\nabla u - \nabla_w u_h, \nabla \times \Phi) \le C s_c^{\frac{1}{2}}(u_h, u_h)\|\nabla \times \Phi\|. \tag{3.6}$$

The a posteriori error estimator is first defined before proving the upper bound estimate of the electrostatic potential ϕ. Let $f_{3,h} \to V_h$ be the L^2 projection of f_3. Then, we introduce a local estimator of ϕ as follows:

$$\eta_{\phi_h,K}^2 = s_{c,K}(\phi_h, \phi_h) + osc^2(f_3, K), \tag{3.7}$$

where $s_{c,K}(\phi_h, \phi_h)$ is defined as in (3.4) and $osc(f_3, K)$ is a high-order local data oscillation if f_3 is smooth enough defined by

$$osc^2(f_3, K) = h_K^2 \|f_3 - f_{3,h}\|_K^2.$$

Let us define a global error estimator and data oscillation as

$$\begin{aligned} \eta_{\phi_h}^2 &= \sum_{K\in\mathcal{T}_h} \eta_{\phi_h,K}^2, \\ osc^2(f_3, \mathcal{T}_h) &= \sum_{K\in\mathcal{T}_h} osc^2(f_3, K). \end{aligned}$$

Now, we are ready to state the following reliability result for the error estimator η_ϕ.

Theorem 3.1. *Let $\phi, p^i \in H_0^1(\Omega)$ be the solutions of* (2.1)-(2.3) *and $\phi_h, p_h^i \in V_h^0$ be the solutions of* (2.8)-(2.9)*. Then, there exists a positive constant C independent of mesh size h such that*

$$|||\phi - \phi_h|||^2 \le C \left(\eta_{\phi_h}^2 + \sum_{i=1}^{2} \left\|p^i - p_{h,0}^i\right\|^2 \right). \tag{3.8}$$

Proof. It follows from (3.2) that

$$\begin{aligned} &\|\nabla\phi - \nabla_w\phi_h\|^2 \\ =& (\nabla\phi - \nabla_w\phi_h, \nabla\phi - \nabla_w\phi_h) \\ =& (\nabla\phi - \nabla_w\phi_h, \nabla\psi) + (\nabla\phi - \nabla_w\phi_h, \nabla\times\Phi). \end{aligned} \tag{3.9}$$

For the first term on the right-hand side of the above equation, by using (2.6), Lemma 2.3 and (2.8), we have

$$\begin{aligned} &(\nabla\phi - \nabla_w\phi_h, \nabla\psi) \\ =& (\nabla\phi, \nabla\psi) - (\nabla_w\phi_h, \nabla\psi) \\ =& (f_3, \psi) + \sum_{i=1}^{2} q^i(p^i, \psi) - \big(\nabla_w\phi_h, \nabla_w(Q_h\psi)\big) \\ =& (f_3, \psi) + \sum_{i=1}^{2} q^i(p^i, \psi) - b_h\big(p_h^i, Q_h\psi\big) + s_c(\phi_h, Q_h\psi) - (f_3, Q_0\psi) \\ =& (f_3, \psi) - (f_3, Q_0\psi) + \sum_{i=1}^{2} q^i(p^i, \psi) - \sum_{i=1}^{2} q^i\big(p_{h,0}^i, \psi\big) \\ &+ \sum_{K\in\mathcal{T}_h} h_K^{-1}\langle \phi_{h,0} - \phi_{h,b}, Q_0\psi - \psi\rangle_{\partial K} \\ =& (f_3 - f_{3,h}, \psi - Q_0\psi) + \sum_{i=1}^{2} q^i\big(p^i - p_{h,0}^i, \psi\big) \\ &+ \sum_{K\in\mathcal{T}_h} h_K^{-1}\langle \phi_{h,0} - \phi_{h,b}, Q_0\psi - \psi\rangle_{\partial K}. \end{aligned}$$

Thus, by the Cauchy-Schwarz inequality, the trace inequality, the property of the projection operator and (3.3), the above equation can be rewritten as

$$
\begin{aligned}
&(\nabla\phi - \nabla_w\phi_h, \nabla\psi) \\
\leq &\sum_{K\in\mathcal{T}_h}\left(\|f_3 - f_{3,h}\|_K\|\psi - Q_0\psi\|_K + \left\|\sum_{i=1}^{2} q^i(p^i - p^i_{h,0})\right\|_K \|\psi\|_K\right) \\
&+ \sum_{K\in\mathcal{T}_h}\left(h_K^{-1}\|\phi_{h,0} - \phi_{h,b}\|^2_{\partial K}\right)^{\frac{1}{2}}\left(h_K^{-1}\|Q_0\psi - \psi\|^2_{\partial K}\right)^{\frac{1}{2}} \\
\leq &C\left(osc(f_3, \mathcal{T}_h) + \left\|\sum_{i=1}^{2} q^i\left(p^i - p^i_{h,0}\right)\right\| + s_c^{\frac{1}{2}}(\phi_h, \phi_h)\right)\|\nabla\psi\| \\
\leq &C\left(osc(f_3, \mathcal{T}_h) + \left\|\sum_{i=1}^{2} q^i\left(p^i - p^i_{h,0}\right)\right\| + s_c^{\frac{1}{2}}(\phi_h, \phi_h)\right)\|\nabla\phi - \nabla_w\phi_h\|. \qquad (3.10)
\end{aligned}
$$

It follows from (3.6) and (3.3) that the second term on the right-hand side of (3.9) becomes

$$
(\nabla\phi - \nabla_w\phi_h, \nabla\times\Phi) \leq Cs_c^{\frac{1}{2}}(\phi_h, \phi_h)\|\nabla\times\Phi\| \leq Cs_c^{\frac{1}{2}}(\phi_h, \phi_h)\|\nabla\phi - \nabla_w\phi_h\|.
$$

Substituting (3.10) and the above estimates into (3.9) and by using Young's inequality, we have

$$
\begin{aligned}
&\|\nabla\phi - \nabla_w\phi_h\|^2 \\
\leq &C\left(osc^2(f_3, \mathcal{T}_h) + s_c(\phi_h, \phi_h) + \left\|\sum_{i=1}^{2} q^i\left(p^i - p^i_{h,0}\right)\right\|^2\right) \\
\leq &C\left(\eta^2_{\phi_h} + \sum_{i=1}^{2}\left\|p^i - p^i_{h,0}\right\|^2\right), \qquad (3.11)
\end{aligned}
$$

where $\eta^2_{\phi_h} = s_c(\phi_h, \phi_h) + osc^2(f_3, \mathcal{T}_h)$.

Now, we easily have

$$
s_c(\phi - \phi_h, \phi - \phi_h) = s_c(\phi_h, \phi_h) \leq \eta^2_{\phi_h}. \qquad (3.12)
$$

Finally, by combining (3.11) and (3.12), it is easy to obtain that (3.8) holds. □

Next, we give the upper bound analysis of the a posteriori error estimators for ion concentrations p^i $(i = 1, 2)$. Let $f_{i,h} \to V_h$ be the L^2 projection of f_i. Then, we introduce a local estimator of p^i as follows:

$$
\eta^2_{p_h^i,K} = s_{c,K}\left(p_h^i, p_h^i\right) + osc^2(f_i, K), \qquad (3.13)
$$

where $s_{c,K}(p_h^i, p_h^i)$ is defined as in (3.4) and $osc(f_i, K)$ is a high-order local data oscillation if f_i is smooth enough defined by

$$
osc^2(f_i, K) = h_K^2\|f_i - f_{i,h}\|^2_K.
$$

Let us define a global error estimator and data oscillation as

$$
\begin{aligned}
\eta^2_{p_h^i} &= \sum_{K\in\mathcal{T}_h}\eta^2_{p_h^i,K}, \\
osc^2(f_i, \mathcal{T}_h) &= \sum_{K\in\mathcal{T}_h} osc^2(f_i, K).
\end{aligned}
$$

The reliability of the error estimator $\eta_{p_h^i}$ defined above is analyzed in the following.

Theorem 3.2. *Let $\phi, p^i \in H_0^1(\Omega)$ be the solutions of (2.1)-(2.3) and $\phi_h, p_h^i \in V_h^0$ be the solutions of (2.8)-(2.9). If $\phi \in W^{k+1,\infty}(\Omega), p^i \in L^\infty(\Omega)$ and the error $e_{p^i,0}$ is small enough, then there exists a positive constant C independent of mesh size h such that*

$$|||p^i - p_h^i|||^2 \le C\left(\eta_{p_h^i}^2 + \eta_{\phi_h}^2 + \sum_{i=1}^{2}\left\|q^i(p^i - p_{h,0}^i)\right\|^2\right). \tag{3.14}$$

Proof. It follows from (3.2) that

$$\begin{aligned}
&\left\|\nabla p^i - \nabla_w p_h^i\right\|^2\\
&= \left(\nabla p^i - \nabla_w p_h^i, \nabla p^i - \nabla_w p_h^i\right)\\
&= \left(\nabla p^i - \nabla_w p_h^i, \nabla\psi\right) + \left(\nabla p^i - \nabla_w p_h^i, \nabla\times\Phi\right).
\end{aligned} \tag{3.15}$$

Using Lemma 2.3, (2.7) and (2.9), we have

$$\begin{aligned}
&\left(\nabla p^i - \nabla_w p_h^i, \nabla\psi\right)\\
&= (\nabla p^i, \nabla\psi) - \left(\nabla_w p_h^i, \nabla\psi\right)\\
&= (f_i, \psi) - q^i(p^i\nabla\phi, \nabla\psi) - \left(\nabla_w p_h^i, \nabla_w(Q_h\psi)\right)\\
&= (f_i, \psi) - q^i(p^i\nabla\phi, \nabla\psi) + q^i\left(p_{h,0}^i\nabla_w\phi_h, \nabla_w(Q_h\psi)\right)\\
&\quad + \sum_{K\in\mathcal{T}_h} h_K^{-1}\left\langle p_{h,0}^i - p_{h,b}^i, Q_0\psi - Q_b\psi\right\rangle_{\partial K} - (f_i, Q_0\psi)\\
&\quad + \sum_{K\in\mathcal{T}_h} h_K^{-1}q^i\left\langle p_{h,0}^i(\phi_{h,0} - \phi_{h,b}), Q_0\psi - Q_b\psi\right\rangle_{\partial K}\\
&= (f_i, \psi - Q_0\psi) - q^i(p^i\nabla\phi, \nabla\psi) + q^i\left(p_{h,0}^i\nabla_w\phi_h, \nabla\psi\right)\\
&\quad + \sum_{K\in\mathcal{T}_h} h_K^{-1}\left\langle p_{h,0}^i - p_{h,b}^i, Q_0\psi - Q_b\psi\right\rangle_{\partial K}\\
&\quad + \sum_{K\in\mathcal{T}_h} h_K^{-1}q^i\left\langle p_{h,0}^i(\phi_{h,0} - \phi_{h,b}), Q_0\psi - Q_b\psi\right\rangle_{\partial K}\\
&= (f_i - f_{i,h}, \psi - Q_0\psi) - q^i\left(p^i\nabla\phi - p_{h,0}^i\nabla_w\phi_h, \nabla\psi\right)\\
&\quad + \sum_{K\in\mathcal{T}_h} h_K^{-1}\left\langle p_{h,0}^i - p_{h,b}^i, Q_0\psi - Q_b\psi\right\rangle_{\partial K}\\
&\quad + \sum_{K\in\mathcal{T}_h} h_K^{-1}q^i\left\langle p_{h,0}^i(\phi_{h,0} - \phi_{h,b}), Q_0\psi - Q_b\psi\right\rangle_{\partial K}\\
&\le \sum_{i=1}^{4}|I_i|.
\end{aligned} \tag{3.16}$$

In the following, we estimate $|I_i|, i = 1, \ldots, 4$. First, for $|I_1|$,

$$\begin{aligned}
|I_1| &= |(f_i - f_{i,h}, \psi - Q_0\psi)|\\
&\le \sum_{K\in\mathcal{T}_h}\|f_i - f_{i,h}\|_K\|\psi - Q_0\psi\|_K\\
&\le C\,osc(f_i, \mathcal{T}_h)\|\nabla\psi\|.
\end{aligned} \tag{3.17}$$

Notably, we shall have

$$\|\nabla\phi\|_{0,\infty,\Omega} \le C, \quad \left\|p_{h,0}^i\right\|_{0,\infty,\Omega} \le C,$$

if $\phi \in W^{k+1,\infty}(\Omega)$, $p^i \in L^\infty(\Omega)$ and the error $e_{p^i,0}$ is small enough [16]. For $|I_2|$, we can obtain

$$\begin{aligned}|I_2| &= \big| -q^i\big(p^i\nabla\phi - p^i_{h,0}\nabla_w\phi_h, \nabla\psi\big)\big| \\ &= \big| -q^i\big(\big(p^i - p^i_{h,0}\big)\nabla\phi + p^i_{h,0}(\nabla\phi - \nabla_w\phi_h), \nabla\psi\big)\big| \\ &\le C\big(\big\|p^i - p^i_{h,0}\big\|\|\nabla\phi\|_{0,\infty,\Omega} + \big\|p^i_{h,0}\big\|_{0,\infty,\Omega}\|\nabla\phi - \nabla_w\phi_h\|\big)\|\nabla\psi\| \\ &\le C\big(\big\|p^i - p^i_{h,0}\big\| + \|\nabla\phi - \nabla_w\phi_h\|\big)\|\nabla\psi\|, \end{aligned} \tag{3.18}$$

Similar to the estimate in Theorem 3.1, for $|I_3|$, we have

$$|I_3| = \left|\sum_{K\in\mathcal{T}_h} h_K^{-1}\langle p^i_{h,0} - p^i_{h,b}, Q_0\psi - Q_b\psi\rangle_{\partial K}\right| \le s_c^{\frac{1}{2}}\big(p^i_h, p^i_h\big)\|\nabla\psi\|. \tag{3.19}$$

By using the inverse inequality on the boundary and the trace inequality, we have

$$\begin{aligned}|I_4| &= \left|\sum_{K\in\mathcal{T}_h} h_K^{-1}q^i\langle p^i_{h,0}(\phi_{h,0} - \phi_{h,b}), Q_0\psi - Q_b\psi\rangle_{\partial K}\right| \\ &\le C\sum_{K\in\mathcal{T}_h}\big\|p^i_{h,0}\big\|_{0,\infty,\partial K}\Big(h_K^{-\frac{1}{2}}\|\phi_{h,0} - \phi_{h,b}\|_{0,\partial K}\Big)\Big(h_K^{-\frac{1}{2}}\|Q_0\psi - \psi\|_{0,\partial K}\Big) \\ &\le C\big\|p^i_{h,0}\big\|_{0,\infty,\Omega}\left(\sum_{K\in\mathcal{T}_h} h_K^{-\frac{1}{2}}\|\phi_{h,0} - \phi_{h,b}\|_{0,\partial K}\right)\left(\sum_{K\in\mathcal{T}_h} h_K^{-\frac{1}{2}}\|Q_0\psi - \psi\|_{0,\partial K}\right) \\ &\le Cs_c^{\frac{1}{2}}(\phi_h, \phi_h)\|\nabla\psi\|. \end{aligned} \tag{3.20}$$

Substituting (3.17)-(3.20) into (3.16), we get

$$\begin{aligned}&\big(\nabla p^i - \nabla_w p^i_h, \nabla\psi\big) \\ &\le C\Big(osc(f_i, \mathcal{T}_h) + s_c^{\frac{1}{2}}\big(p^i_h, p^i_h\big) + \big\|p^i - p^i_{h,0}\big\| + s_c^{\frac{1}{2}}(\phi_h, \phi_h) + \|\nabla\phi - \nabla_w\phi_h\|\Big)\|\nabla\psi\| \\ &\le C\Big(osc(f_i, \mathcal{T}_h) + s_c^{\frac{1}{2}}\big(p^i_h, p^i_h\big) + \big\|p^i - p^i_{h,0}\big\| + |\!|\!|\phi - \phi_h|\!|\!|\Big)\|\nabla\psi\|. \end{aligned} \tag{3.21}$$

Hence, from Theorems 3.1 and (3.3), the above equation can be rewritten as

$$\begin{aligned}&\big(\nabla p^i - \nabla_w p^i_h, \nabla\psi\big) \\ &\le C\left(osc(f_i, \mathcal{T}_h) + s_c^{\frac{1}{2}}\big(p^i_h, p^i_h\big) + \big\|p^i - p^i_{h,0}big\| + \eta_{\phi_h} + \sum_{i=1}^{2}\big\|q^i(p^i - p^i_{h,0})\big\|\right)\|\nabla\psi\| \\ &\le C\left(osc(f_i, \mathcal{T}_h) + s_c^{\frac{1}{2}}\big(p^i_h, p^i_h\big) + \eta_{\phi_h} + \sum_{i=1}^{2}\big\|q^i(p^i - p^i_{h,0})\big\|\right)\big\|\nabla p^i - \nabla_w p^i_h\big\|. \end{aligned} \tag{3.22}$$

It follows from Lemma 3.2 and (3.3) that

$$\begin{aligned}&\big(\nabla p^i - \nabla_w p^i_h, \nabla\times\Phi\big) \\ &\le Cs_c^{\frac{1}{2}}\big(p^i_h, p^i_h\big)\|\nabla\times\Phi\| \\ &\le Cs_c^{\frac{1}{2}}\big(p^i_h, p^i_h\big)\big\|\nabla p^i - \nabla_w p^i_h\big\|. \end{aligned} \tag{3.23}$$

Substituting (3.22)-(3.23) into (3.15) and by using Young's inequality, we have

$$\begin{aligned}
&\left\|\nabla p^i - \nabla_w p_h^i\right\|^2 \\
&\leq C\left(osc^2(f_i, \mathcal{T}_h) + s_c\big(p_h^i, p_h^i\big) + \eta_{\phi_h}^2 + \sum_{i=1}^{2} \left\|q^i(p^i - p_{h,0}^i)\right\|^2 \right) \\
&\leq C\left(\eta_{p_h^i}^2 + \eta_{\phi_h}^2 + \sum_{i=1}^{2} \left\|q^i(p^i - p_{h,0}^i)\right\|^2 \right).
\end{aligned} \tag{3.24}$$

where $\eta_{p^i}^2 = osc^2(f_i, \mathcal{T}_h) + s_c(p_h^i, p_h^i)$.

Next, similar to Theorem 3.1, we can easily obtain

$$s_c\big(p^i - p_h^i, p^i - p_h^i\big) = s_c\big(p_h^i, p_h^i\big) \leq \eta_{p_h^i}^2.$$

Combining (3.24) with the above inequality, it follows that

$$|||p^i - p_h^i|||^2 \leq C\left(\eta_{p_h^i}^2 + \eta_{\phi_h}^2 + \sum_{i=1}^{2} \left\|q^i(p^i - p_{h,0}^i)\right\|^2 \right). \tag{3.25}$$

It is proved that (3.14) holds.

Remark 3.2. Form Theorems 3.1 and 3.2, if $\phi \in W^{k+1,\infty}(\Omega), p^i \in L^\infty(\Omega)$ and $\|e_{p^i,0}\| \leq Ch^{k+1}$ holds, then we have

$$|||\phi - \phi_h|||^2 \leq C\big(\eta_{\phi_h}^2 + h^{2(k+1)}\big), \tag{3.26}$$

$$|||p^i - p_h^i|||^2 \leq C\big(\eta_{p_h^i}^2 + \eta_{\phi_h}^2 + h^{2(k+1)}\big). \tag{3.27}$$

Note that (3.26) and (3.27) in hold based on the assumption $\|e_{p^i,0}\| \leq Ch^{k+1}$. The L^2 norm error estimate of p^i holds when the WG finite element method is used to solve the time-dependent PNP equations (see [18, Theorem 4.3]). For the steady-state PNP equations, it is difficult to derive the L^2 norm error estimate of p^i by using the traditional Aubin-Nitsche duality technique due to their strong coupling. Although this assumption cannot be proved theoretically, numerical results show that the error convergence order of p^i in the L^2 norm can reach $\mathcal{O}(h^{k+1})$. (see Figs. 4.4, 4.7, 4.10 and 4.13 in Example 4.1).

3.2. Lower bound

In this subsection, local lower bound estimates for the a posteriori error estimators for the electrostatic potential ϕ and ion concentrations p^i are presented. The upper bound results indicate the reliability of the estimators, while the lower bound results indicate the effectiveness of the estimators. From the constructed a posteriori error estimators and the characteristics of the energy norm, the local lower bounds for the a posteriori error estimators can be easily obtained.

Let us define the energy norm on each element K as follows:

$$|||v_h|||_K^2 = (\nabla_w v_h, \nabla_w v_h)_K + s_{c,K}(v_h, v_h). \tag{3.28}$$

According to the definition of the local energy norm $|||v_h|||_K^2$, it can be seen that the local stability term $s_{c,K}(v_h, v_h)$ is only part of it. Therefore, the local lower bound estimate of ϕ can be obtained from the definition (3.7) of the local error estimator of ϕ.

Theorem 3.3. *Let p^i, $\phi \in H_0^1(\Omega)$ and $p_h^i, \phi_h \in V_h^0$ be the solutions of* (2.1)-(2.3) *and* (2.8)-(2.9)*, respectively. The local error estimator $\eta_{\phi_h,K}$ of ϕ satisfies*

$$\eta_{\phi_h,K}^2 \leq \|\nabla\phi - \nabla_w \phi_h\|_K + osc^2(f_3, K).$$

Proof. It follows from (3.7) and (3.28) that we have

$$\begin{aligned}\eta_{\phi_h,K}^2 &= s_{c,K}(\phi_h, \phi_h) + osc^2(f_3, K)\\ &\leq \|\nabla\phi - \nabla_w \phi_h\|_K + s_{c,K}(\phi_h, \phi_h) + osc^2(f_3, K)\\ &\leq \|\phi - \phi_h\|_K + osc^2(f_3, K),\end{aligned}$$

where $\eta_{\phi_h,K}$ is defined as (3.7). This completes the proof. □

Similarly, it is easy to obtain the local a posteriori error estimator $\eta_{p_h^i,K}$ of p^i defined in (3.13) that satisfies the following lower bound estimate.

Theorem 3.4. *Let $p^i, \phi \in H_0^1(\Omega)$ and $p_h^i, \phi_h \in V_h^0$ be the solutions of* (2.1)-(2.3) *and* (2.8)-(2.9)*, respectively. The local error estimator $\eta_{p_h^i,K}$ of p^i satisfies*

$$\eta_{p_h^i,K}^2 \leq \left\|\nabla p^i - \nabla_w p_h^i\right\|_K + osc^2(f_i, K). \tag{3.29}$$

Proof. It follows from (3.13) and (3.28) that we have

$$\begin{aligned}\eta_{p_h^i,K}^2 &= s_{c,K}\left(p_h^i, p_h^i\right) + osc^2(f_i, K)\\ &\leq \left\|\nabla p^i - \nabla_w p_h^i\right\|_K + s_{c,K}\left(p_h^i, p_h^i\right) + osc^2(f_i, K)\\ &\leq \left\|p^i - p_h^i\right\|_K + osc^2(f_i, K),\end{aligned}$$

where $\eta_{p_h^i,K}$ is defined as (3.13). This completes the proof. □

4. Numerical Experiment

In this section, the corresponding adaptive algorithm is designed to verify the effectiveness and reliability of the constructed a posteriori error estimators. In numerical calculations, we take $k = 1$ in the WG finite element space V_h. To verify the flexibility of the WGFEM on mesh, different mesh refinement strategies are used for the adaptive algorithm in numerical calculation. We design the corresponding adaptive algorithm to solve the PNP equations.

Given an initial mesh $\mathcal{T}_h$, an associated finite element space V_h and a tolerance TOL, the typical adaptive algorithm is then designed as follows. In step 3, the Dörfler strategy [7] is used to mark the elements that need to be refined. The method of refining the mesh is referred to in [10–12], and the refinement parameter is $\lambda = 0.5$ in the adaptive algorithm.

In the following, Algorithm 4.1 is used to solve the PNP system (2.1)-(2.3) with singularity at the origin. The computational domains are $\Omega = [0, 1]^2 \in R^2$ and $q^1 = 1, q^2 = -1$.

Example 4.1. Let us consider the steady-state PNP equation (2.1)-(2.3). The boundary condition and the right-hand side functions are chosen such that the exact solution (ϕ, p^1, p^2) is given by

$$\begin{aligned}\phi(x, y) &= \frac{(x - x^2)(y - y^2)}{x^2 + y^2},\\ p^1(x, y) &= 1 - e^{\phi},\\ p^2(x, y) &= 1 - e^{-\phi}.\end{aligned}$$

Algorithm 4.1: Adaptive Algorithm for Steady-state PNP Equations.

Step 1. WG finite element solution computing. Find the WG finite element solutions $\phi_h = \{\phi_{h,0}, \phi_{h,b}\} \in V_h^0$ and $p_h^i = \{p_{h,0}^i, p_{h,b}^i\} \in V_h^0$ for the WG discrete scheme (2.8)-(2.9).

Step 2. Error estimation. For all elements $K \in \mathcal{T}_h$, the local error estimators $\eta_{\phi_h,K}$, $\eta_{p_h^i,K}$ are computed by (3.7) and (3.13).

Step 3. Local refinement. If $(\sum_{K\in\mathcal{T}_h} \eta^2_{\phi_h,K})^{1/2} > TOL$ or $(\sum_{K\in\mathcal{T}_h} \eta^2_{p_h^i,K})^{1/2} > TOL$, for all $K \in \mathcal{T}_h$, refine those elements that satisfy $\eta_{\phi_h,K} \geq \lambda \max\{\eta_{\phi_h,K},\ \eta_{p_h^i,K}\}$ or $\eta_{p_h^i,K} \geq \lambda \max\{\eta_{\phi_h,K},\ \eta_{p_h^i,K}\}$, where $\lambda \in (0,1)$ is a given refinement parameter.

Step 4. Generate a new mesh. Generate a new mesh $\mathcal{T}_h$ and WG finite element space V_h, and return to **Step 1**. Otherwise, the computation is terminated.

Algorithm 4.1 is used to compute several different shapes of adaptive meshes, namely, triangular meshes, quadrilateral meshes, triangular meshes with hanging points and quadrilateral meshes with hanging points. The triangular meshes with hanging points and the quadrilateral meshes with hanging points are regarded as mixed polygonal meshes in numerical calculation. For example, if a triangular element has a hanging point, the element is regarded as a quadrilateral. Fig. 4.1 shows the initial mesh of triangles and triangles with hanging points, and Fig. 4.2 shows the initial mesh of quadrilaterals and quadrilaterals with hanging points, where $DOFs$ represents the mesh node degrees of freedom.

We first show the numerical results of the adaptive computation on the triangular meshes. Fig. 4.3 shows the final triangle adaptive mesh generated by Algorithm 4.1. The refinement concentrates on the origin in Fig. 4.3, which matches the singularity of the numerical solutions. Fig. 4.4 shows the L^2 norm for p^1 and p^2 on the triangular adaptive meshes. Fig. 4.5 shows the a posteriori error estimators and the energy norms of the error obtained for ϕ, p^1 and p^2 on the triangular adaptive meshes, respectively.

In Figs. 4.4 and 4.5, $DOFs$ of the mesh is used instead of the mesh size h to show the error convergence order; that is, for the two-dimensional problem, $O(DOFs^{-1})$ means that

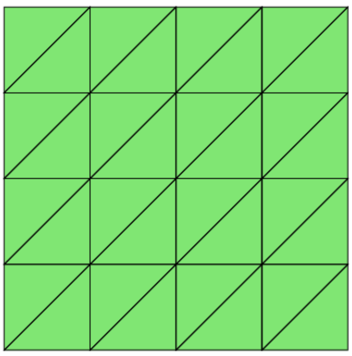

Fig. 4.1. Triangular initial mesh, $DOFs = 25$.

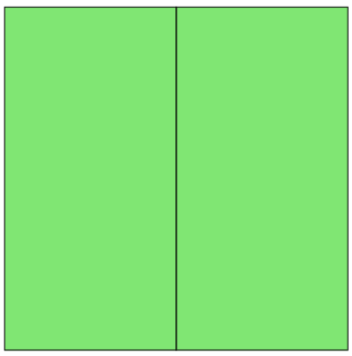

Fig. 4.2. Quadrilateral initial mesh, $DOFs = 2$.

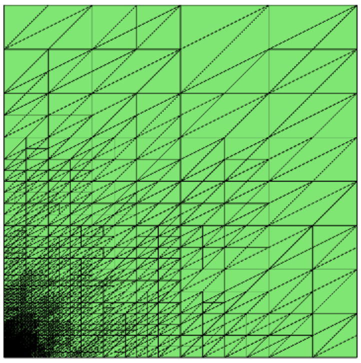

Fig. 4.3. Triangle adaptive mesh, $DOFs = 6580$.

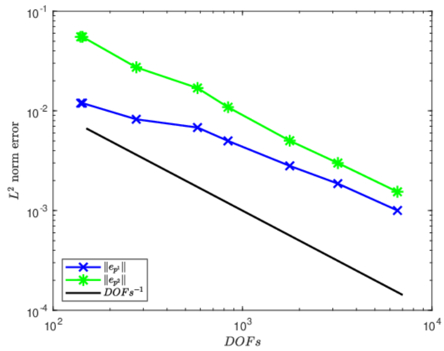

Fig. 4.4. The L^2 norms of p^1 and p^2 on the triangle adaptive meshes.

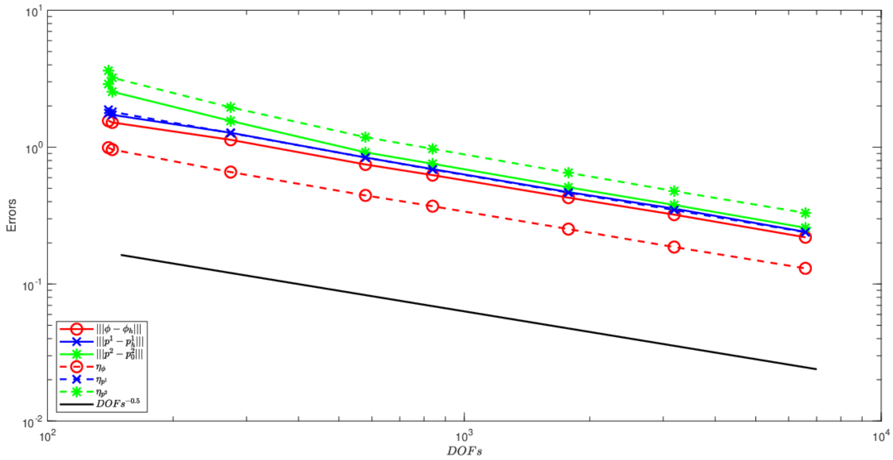

Fig. 4.5. The a posteriori error estimators and the energy norms of ϕ, p^1 and p^2 on triangle adaptive meshes.

the convergence order is $\mathcal{O}(h^2)$. Fig. 4.4 shows the error convergence orders of the errors $e_{p^i,0}$ $(i = 1, 2)$ in the L^2 norm between the L^2 projection $Q_0 p^i$ of the exact solutions p^i and the WG finite element solutions p_h^i on the triangular adaptive meshes. The slope of the convergence curve of the error $e_{p^i,0}$ on the triangular adaptive meshes is close to -1, which indicates that the orders of convergence are second order, i.e. $\mathcal{O}(h^2)$. This validates the hypothesis in Theorems 3.1 and 3.2. As seen from Fig. 4.5, the slopes of the convergence curves of the a posteriori error estimators and the energy norms of the errors of ϕ, p^1 and p^2 on the triangular adaptive meshes are close to -0.5, which indicates that the convergence order is $\mathcal{O}(h)$, that is, first order. Figs. 4.4 and 4.5 show that the L^2 norms of the errors of p^i are higher order than those of the a posteriori error estimators.

Next, the numerical results computed on the quadrilateral meshes are presented. The quadrilateral adaptive mesh obtained by Algorithm 4.1 is shown in Fig. 4.6. Similar to Fig. 4.3, the estimators can accurately detect the singularity and add refinement focused at the point $(0, 0)$.

The numerical results for the L^2 norms of p^1 and p^2 are given in Fig. 4.7. Their convergence orders are all $O(h^2)$. Fig. 4.8 shows the numerical results for the a posteriori error estimators

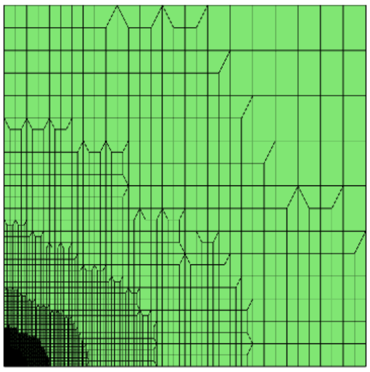

Fig. 4.6. Quadrilateral adaptive mesh, $DOFs = 13601$.

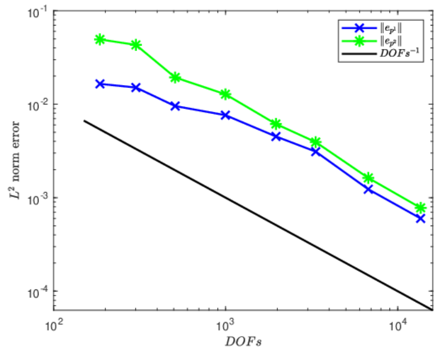

Fig. 4.7. The L^2 norms of p^1 and p^2 on the quadrilateral adaptive meshes.

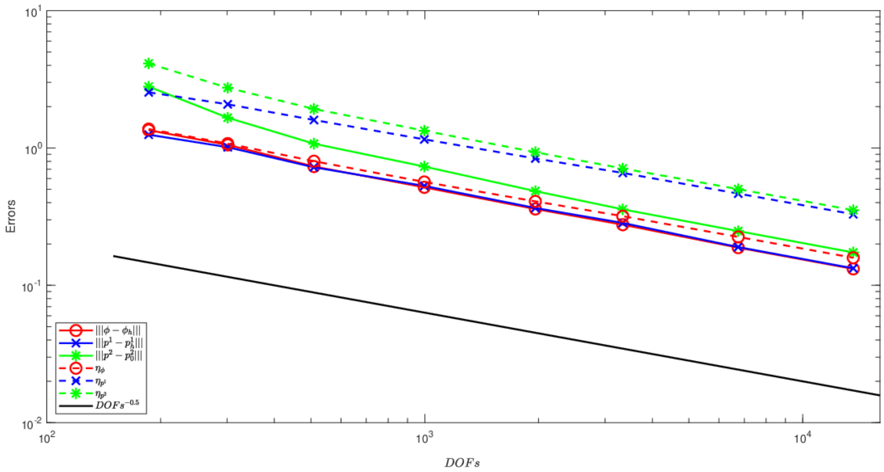

Fig. 4.8. The a posteriori error estimators and the energy norms of ϕ, p^1 and p^2 on quadrilateral adaptive meshes.

and the energy norms of the error obtained for ϕ, p^1 and p^2 on the quadrilateral adaptive meshes, respectively. Their convergence orders are all $\mathcal{O}(h)$. They both achieve the desired optimal convergence rates.

Finally, numerical results computed on the triangular adaptive meshes with hanging points and the quadrilateral adaptive meshes with hanging points are presented. We give the triangular adaptive mesh with hanging points and the quadrilateral adaptive mesh with hanging points in Figs. 4.9 and 4.12, respectively. As Figs. 4.9 and 4.12 show that the refinement is focused at the origin $(0, 0)$. These results indicate that the a posteriori estimators can capture the singularity accurately.

We also plot the L^2 norms of errors in Figs. 4.10 and 4.13, while that of the decay of the a posteriori estimators and energy norms of errors in Figs. 4.11 and 4.14. We can still observe that Algorithm 4.1 achieves optional convergence orders for the a posteriori estimators, energy norms and L^2 norms of the errors. The convergence results agree with our theoretical conclusions.

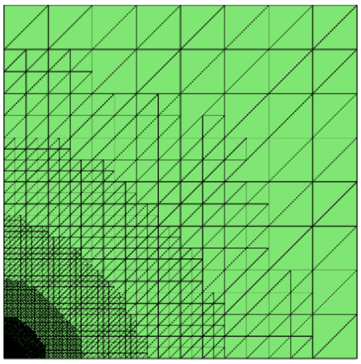

Fig. 4.9. Triangle adaptive mesh with hanging points, $DOFs = 7433$.

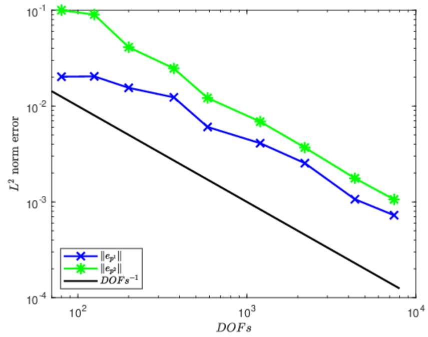

Fig. 4.10. The L^2 norms of p^1 and p^2 on the triangle adaptive meshes with hanging points.

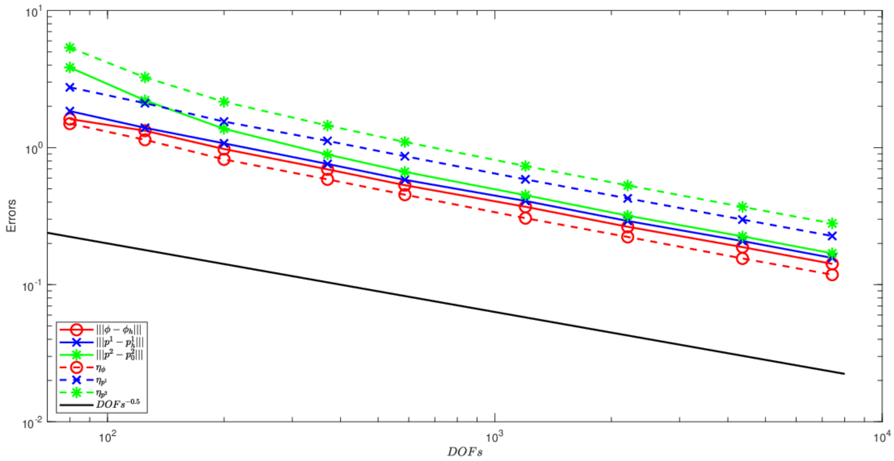

Fig. 4.11. The a posteriori error estimators and the energy norms of ϕ, p^1 and p^2 on the triangle adaptive meshes with hanging points.

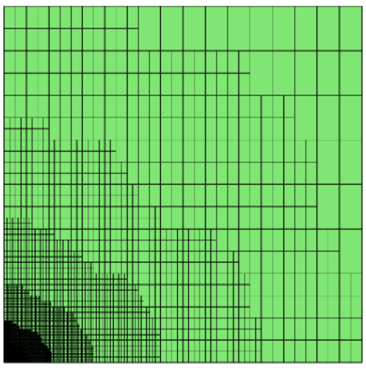

Fig. 4.12. Quadrilateral adaptive mesh with hanging points, $DOFs = 15041$.

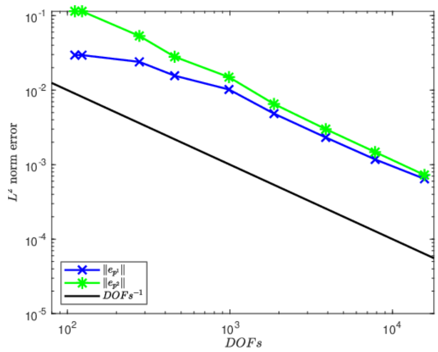

Fig. 4.13. The L^2 norms of p^1 and p^2 on quadrilateral adaptive meshes with hanging points.

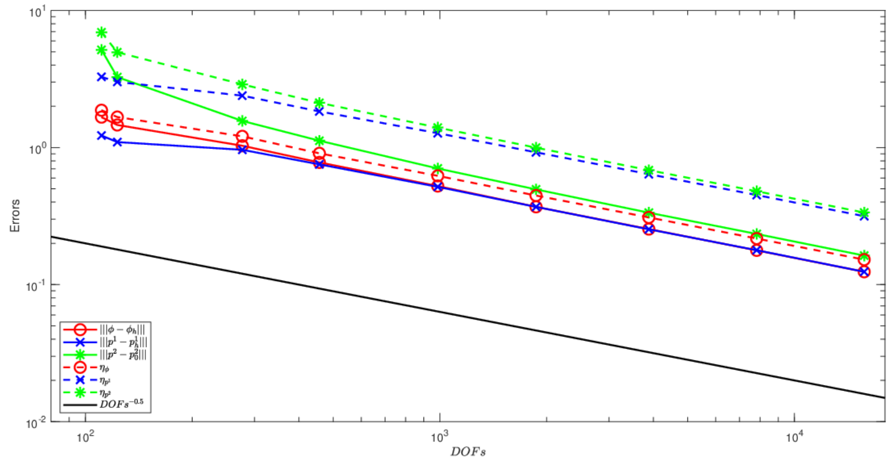

Fig. 4.14. The a posteriori error estimators and the energy norms of ϕ, p^1 and p^2 on quadrilateral adaptive meshes with hanging points.

5. Conclusion

In this paper, a posteriori error estimation for a class of steady-state PNP equations is proposed that uses the WGFEM. We construct a posteriori error estimators of electrostatic potential and ion concentrations; then, we prove the reliability and efficiency of the a posteriori error estimators. We validate the theoretical analysis by numerical experiments on triangular, quadrilateral and polygonal meshes with hanging nodes. The numerical results show that the a posteriori error estimators can locate the singularity accurately and can conduct the refinement effectively. Our a posteriori error estimators are simple in form and implementation, which makes them realistic in practical applications.

Acknowledgments. We would like to thank Professor Waixiang Cao for useful discussion.

G. Ji is partially supported by the National Natural Science Foundation of China (Grant No. 12471363).

References

[1] J.H. Adler, X. Hu, L. Mu, and X. Ye, An a posteriori error estimator for the weak Galerkin least-squares finite-element method, *J. Comput. Appl. Math.*, **362** (2019), 383–399.

[2] F. Bao, L. Mu, and J. Wang, A fully computable a posteriori error estimate for the Stokes equations on polytopal meshes, *SIAM J. Numer. Anal.*, **57**:1 (2019), 458–477.

[3] M. Bessemoulin-Chatard and C. Chainais-Hillairet, Uniform-in-time bounds for approximate solutions of the drift-diffusion system, *Numer. Math.*, **141** (2019), 881–916.

[4] L. Chen, J. Wang, and X. Ye, A posteriori error estimates for weak Galerkin finite element methods for second order elliptic problems, *J. Sci. Comput.*, **59**:2 (2014), 496–511.

[5] Y. Chen and T. Zhang, A weak Galerkin finite element method for Burgers' equation, *J. Comput. Appl. Math.*, **348** (2019), 103–119.

[6] R.D. Coalson and M.G. Kurnikova, Poisson-Nernst-Planck theory approach to the calculation of current through biological ion channels, *IEEE Trans. Nanobiosci.*, **4**:1 (2005), 81–93.

[7] W. Dörfler, A convergent adaptive algorithm for Poisson's equation, *SIAM J. Numer. Anal.*, **33**:3 (1996), 1106–1124.

[8] Y. Du and Z. Zhang, A numerical analysis of the weak Galerkin method for the Helmholtz equation with high wave number, *Commun. Comput. Phys.*, **22**:1 (2017), 133–156.

[9] R.G. Durán, Mixed finite element methods, in: *Mixed Finite Elements, Compatibility Conditions, and Applications. Lecture Notes in Mathematics*, Vol. 1939, Springer, (2008), 1–44.

[10] S. Funken, D. Praetorius, and P. Wissgott, Efficient implementation of adaptive P1-FEM in Matlab, *Comput. Methods Appl. Math.*, **11**:4 (2011), 460–490.

[11] S. Funken and A. Schmidt, Efficient implementation of adaptive mesh refinement in 2D, `https://github.com/aschmidtuulm/ameshref`, 2018.

[12] S.A. Funken and A. Schmidt, Adaptive mesh refinement in 2D-An efficient implementation in Matlab, *Comput. Methods Appl. Math.*, **20**:3 (2020), 459–479.

[13] H. Gao and D. He, Linearized conservative finite element methods for the Nernst-Planck-Poisson equations, *J. Sci. Comput.*, **72**:3 (2017), 1269–1289.

[14] Z. Gharibi, M. Dehghan, and M. Abbaszadeh, Numerical analysis of locally conservative weak Galerkin dual-mixed finite element method for the time-dependent Poisson-Nernst-Planck system, *Comput. Math. Appl.*, **92** (2021), 88–108.

[15] V. Girault and P. Raviart, *Finite Element Methods for Navier-Stokes Equations: Theory and Algorithms*, in: Springer Series in Computational Mathematics, Vol. 5, Springer, 1986.

[16] T. Hao, M. Ma, and X. Xu, Adaptive finite element approximation for steady-state Poisson-Nernst-Planck equations, *Adv. Comput. Math.*, **48**:4 (2022), 49.

[17] D. He and K. Pan, An energy preserving finite difference scheme for the Poisson-Nernst-Planck system, *Appl. Math. Comput.*, **287** (2016), 214–223.

[18] G. Ji and W. Zhu, A weak Galerkin finite element method for time-dependent Poisson-Nernst-Planck equations, *J. Comput. Appl. Math.*, **416** (2022), 114563.

[19] H. Li, A posteriori error estimates for the weak Galerkin finite element methods on polytopal meshes, *Commun. Comput. Phys.*, **26**:2 (2019), 558–578.

[20] G. Lin, J. Liu, and F. Sadre-Marandi, A comparative study on the weak Galerkin, discontinuous Galerkin, and mixed finite element methods, *J. Comput. Appl. Math.*, **273** (2015), 346–362.

[21] W. Liu, One-dimensional steady-state Poisson-Nernst-Planck systems for ion channels with multiple ion species, *J. Differential Equations*, **246**:1 (2009), 428–451.

[22] X. Liu, J. Li, and Z. Chen, A weak Galerkin finite element method for the Navier-Stokes equations, *J. Comput. Appl. Math.*, **333** (2018), 442–457.

[23] Y. Liu, G. Wang, M. Wu, and Y. Nie, A recovery-based a posteriori error estimator of the weak Galerkin finite element method for elliptic problems, *J. Comput. Appl. Math.*, **406** (2022), 113926.

[24] M. Mock, On equations describing steady-state carrier distributions in a semiconductor device, *Comm. Pure Appl. Math.*, **25**:6 (1972), 781–792.

[25] L. Mu, Weak Galerkin based a posteriori error estimates for second order elliptic interface problems on polygonal meshes, *J. Comput. Appl. Math.*, **361** (2019), 413–425.

[26] L. Mu, J. Wang, Y. Wang, and X. Ye, A computational study of the weak Galerkin method for second-order elliptic equations, *Numer. Algorithms*, **63** (2013), 753–777.

[27] L. Mu, J. Wang, and X. Ye, A weak Galerkin finite element method with polynomial reduction, *J. Comput. Appl. Math.*, **285** (2015), 45–58.

[28] L. Mu, J. Wang, and X. Ye, Weak Galerkin finite element methods on polytopal meshes, *Int. J. Numer. Anal. Model.*, **12**:1 (2015), 31–53.

[29] R. Shen, S. Shu, Y. Yang, and M. Fang, Gradient recovery-type a posteriori error estimates for steady-state Poisson-Nernst-Planck equations, *Adv. Appl. Math. Mech.*, **12**:6 (2020), 1353–1383.

[30] S. Shields, J. Li, and E.A. Machorro, Weak Galerkin methods for time-dependent Maxwell's equations, *Comput. Math. Appl.*, **74**:9 (2017), 2106–2124.

[31] A. Singer and J. Norbury, A Poisson-Nernst-Planck model for biological ion channels – an asymptotic analysis in a three-dimensional narrow funnel, *SIAM J. Appl. Math.*, **70**:3 (2009), 949–968.

[32] B. Tu, M. Chen, Y. Xie, L. Zhang, B. Eisenberg, and B. Lu, A parallel finite element simulator for

ion transport through three-dimensional ion channel systems, *J. Comput. Chem.*, **34**:24 (2013), 2065–2078.

[33] R. Verfürth, *A Posteriori Error Estimation Techniques for Finite Element Methods*, Oxford University Press, 2013.

[34] J. Wang and X. Ye, A weak Galerkin finite element method for second-order elliptic problems, *J. Comput. Appl. Math.*, **241** (2013), 103–115.

[35] J. Wang and X. Ye, A weak Galerkin mixed finite element method for second order elliptic problems, *Math. Comp.*, **83**:289 (2014), 2101–2126.

[36] J. Wang and X. Ye, A weak Galerkin finite element method for the Stokes equations, *Adv. Comput. Math.*, **42** (2016), 155–174.

[37] Y. Xie, J. Cheng, B. Lu, and L. Zhang, Parallel adaptive finite element algorithms for solving the coupled electro-diffusion equations, *Comput. Math. Biophys.*, **1** (2013), 90–108.

[38] S. Xu, M. Chen, S. Majd, X. Yue, and C. Liu, Modeling and simulating asymmetrical conductance changes in gramicidin pores, *Comput. Math. Biophys.*, **2**:1 (2014), 34–55.

[39] Y. Yang and B. Lu, An error analysis for the finite element approximation to the steady-state Poisson-Nernst-Planck equations, *Adv. Appl. Math. Mech.*, **5**:1 (2013), 113–130.

[40] Y. Yang, R. Shen, M. Fang, and S. Shu, Local averaging type a posteriori error estimates for the nonlinear steady-state Poisson-Nernst-Planck equations, *J. Comput. Appl. Math.*, **404** (2022), 113874.

[41] S.Y. Yi, A lowest-order weak Galerkin method for linear elasticity, *J. Comput. Appl. Math.*, **350** (2019), 286–298.

[42] Q. Zhai, H. Xie, R. Zhang, and Z. Zhang, The weak Galerkin method for elliptic eigenvalue problems, *Commun. Comput. Phys.*, **26**:1 (2019), 160–191.

[43] Q. Zhai and R. Zhang, Lower and upper bounds of Laplacian eigenvalue problem by weak Galerkin method on triangular meshes, *Discrete Contin. Dyn. Syst. Ser. B*, **24**:1 (2019), 403–413.

[44] J. Zhang, J. Li, J. Li, and K. Zhang, An adaptive weak Galerkin finite element method with hierarchical bases for the elliptic problem, *Numer. Methods Partial Differential Equations*, **36**:6 (2020), 1280–1303.

[45] X. Zheng and X. Xie, A posteriori error estimator for a weak Galerkin finite element solution of the Stokes problem, *East Asian J. Appl. Math.*, **7**:3 (2017), 508–529.

[46] W. Zhu, Y. Yang, G. Ji, and B. Lu, Residual type a posteriori error estimates for the time-dependent Poisson-Nernst-Planck equations, *J. Sci. Comput.*, **90** (2022), 1–35.